Review

https://doi.org/10.23934/2223-9022-2022-11-2-332-346

Imaging of Septic Pulmonary Embolism in Right-Side Infective Endocarditis

***A.S. Vinokurov*[1, 2, 3] ✉, *N.S. Chipigina*[1], *Yu.R. Zyuzya*[4, 5], *A.L. Yudin*[1]**

Radiology Departments
[1] N.I. Pirogov Russian National Research Medical University
1, Ostrovityanov St., Moscow, 117997, Russian Federation
[2] V.P. Demikhov City Hospital of Moscow City Health Department
4, Shkuleva St., Moscow, 109263, Russian Federation
[3] Moscow Multidisciplinary Clinical Center «Kommunarka»
8, Sosenskiy Stan St., Moscow, Sosenskoe, Kommunarka, 108814, Russian Federation
[4] Infectious Diseases Clinical Hospital №2
15, 8-Sokolinoy Gory St., Moscow,105275, Russian Federation
[5] Moscow Research and Clinical Center for Tuberculosis Control
10, Stromynka St., 107014, Moscow, Russian Federation
[6] National Medical Research Centre of Phthisiopulmonology and Infection Diseases
4, bldg. 2, Dostoevskogo St., 127994, Moscow, Russian Federation

✉ **Contacts:** Anton S. Vinokurov, Radiologist, Radiology Departments of V.P. Demikhov City Hospital. Email: antonvin.foto@gmail.com

ABSTRACT Early and correct diagnosis of infective endocarditis (IE) of the right heart does not lose its importance due to the persistence of the problem of intravenous drug use and an increase in the number of surgical interventions on the heart. Septic pulmonary embolism (SPE) is a typical sign of right-side IE, and, with a number of nonspecific respiratory symptoms in patients with fever, its detection by radiology allows to start a diagnostic search for IE and locate the primary embolic source in the right parts of the heart. The review examines the current state of the problem of right-side IE, morphology and clinical evidence, main CT signs and differential diagnostics of SPE, including the context of the COVID-19 pandemic.

Keywords: infective endocarditis, septic pulmonary embolism, lung infarction, lung cavities, COVID-19, CT

For citation Vinokurov AS, Chipigina NS, Zyuzya YuR, Yudin AL. Imaging of Septic Pulmonary Embolism in Right-Side Infective Endocarditis. *Russian Sklifosovsky Journal of Emergency Medical Care.* 2022;11(2):332–346. https://doi.org/10.23934/2223-9022-2022-11-2-332-346 (in Russ.)

Conflict of interest Authors declare lack of the conflicts of interests

Acknowledgments, sponsorship The study has no sponsorship

Affiliations

Anton S. Vinokurov	Radiologist, Radiology departments of Demikhov City Hospital and Moscow Multidisciplinary Clinical Center «Kommunarka», Assistant Professor, Department of Radiation Diagnostics and Therapy, Pirogov Russian National Research Medical University; https://orcid.org/0000-0002-0745-3438, antonvin.foto@gmail.com; 30%, concept of the article, collection and processing of material, text writing, preparation of radiology images
Natalya S. Chipigina	Candidate of Medical Sciences, Associate Professor, A.I. Nesterov Faculty Therapy Department, Pirogov Russian National Research Medical University; https://orcid.org/0000-0002-2083-0437, chipigina-natalia56@yandex.ru; 30%, concept of the article, collection and processing of material, text writing, editing
Yulia R. Zyuzya	Candidate of Medical Sciences, Pathologist, Centralized Patholology Department, Moscow Research and Clinical Center for Tuberculosis Control, National Medical Research Centre of Phthisiopulmonology and Infection Diseases; https://orcid.org/0000-0003-2814-4826, ms.vodova@mail.ru; 25%, text writing, preparation of images of macro- and micro-histology items
Andrey L. Yudin	Doctor of Medical Sciences, Professor, Head, Radiology Department, Pirogov Russian National Research Medical University https://orcid.org/ 0000-0002-0310-0889, prof_yudin@mail.ru; 15%, the concept of the work, approval of the final version of the article

IE – Infective endocarditis
PET – Positron emission tomography
CT – Computed tomography
SPE – Septic pulmonary embolism
Echo – Echocardiography
TV – Tricuspid valve
ARDS – Acute respiratory distress syndrome
UIP – Usual interstitial pneumonia
NSIP – Nonspecific interstitial pneumonia
PE – Pulmonary embolism

Infective endocarditis (IE) of the right heart is observed less frequently than left-sided IE and ranges from 5 to 51.9% of IE cases in different countries, depending primarily on the prevalence of drug addiction, the main risk factor for infection of the right heart [1-7]. In the Russian Federation, right-sided localization is observed in about one third of IE cases [8].

Most often right-sided IE affects the tricuspid valve (85-100% of drug addicts and 56-82% of cases not associated with drug addiction), less often the pulmonary valve (3-20.5% of patients with right-sided IE), and very rarely its localization is parietal, in the coronary sinus, on the Thebesian valve, Eustachian valve or Chiari network [1, 4, 7, 9-13].

The prevailing localization in the right parts of the heart (up to 92.3%) is most typical for IE of injection drug addicts; right-sided IE is also typical for patients with a permanent pacemaker [1, 7, 14, 15]. Much less often, right-sided IE is associated with adults prone to congenital heart defects – a ventricular septal defect, atrial septal defect, tetralogy of Fallot, patent ductus arteriosus. It also occurs on a prosthetic valve, or, as a relapse, on a native valve previously affected by IE [1, 13]. Intravenous catheters and long term hemodialysis predispose to IE of the right heart; cases of right-sided IE in patients without any risk factors are described very rarely [12, 13, 16].

A reliable diagnosis of IE in accordance with the current diagnostic criteria (Duke criteria) is based on the visualization of typical "fresh" endocardial vegetations and new destruction of the affected valves visualized during echocardiography (echo) or positron emission computed tomography (PET-CT) of the heart, as well as on the isolation of typical pathogens in a blood culture test [17]. However, at the prehospital stage of the disease, these necessary examinations are performed in less than a third of patients [18].

Auscultation of a new murmur of valvular regurgitation, which occurs during the formation of valvular insufficiency as a result of destructive changes in the leaflets, is considered a predictor of IE, but in 50-80% of patients with right-sided IE, the murmur appears late or is not heard at all [18-21]. At the onset and in the first weeks of right-sided IE, nonspecific symptoms predominate: fever with chills in 95-97.1% of patients and "the lung mask" – respiratory manifestations caused by septic pulmonary embolism (SPE) which develops during fragmentation of vegetations containing colonies of microorganisms and spread of infected emboli in the pulmonary arteries [15, 18, 21, 22].

PATHOMORPHOLOGICAL PICTURE AND CLINICAL MANIFESTATIONS OF SPE IN PATIENTS WITH RIGHT-SIDED IE

SPE is observed in 53-100% of patients with right-sided IE, the lesion is usually bilateral, often multiple and recurrent [3, 15]. Thrombi containing colonies of microorganisms cause mechanical obstruction of predominantly secondary branches of the pulmonary artery with the formation of areas of infarction of the lung tissue, infectious inflammation and an abscess as a result of the lung tissue collapse.

Reddish-cyanotic or brownish-red moderately compacted foci of hemorrhagic infarcts of various sizes (depending on the caliber of the obturated blood vessel) are macroscopically identified in the lung. In most cases, these are infarcted areas of the lung of an irregular triangular shape, the base facing the pleura, the apex - the root of the lung. In the infarcted area of the lung, sequestration of necrotic masses occurs with the subsequent formation of a destructive cavity (Fig. 1) and suppuration of necrotic masses of hemorrhagic infarction with abscess formation. The walls of the abscess are usually yellowish-brown in color. Piemic foci may be microscopically small and can be detected only by histological examination (Fig. 2)

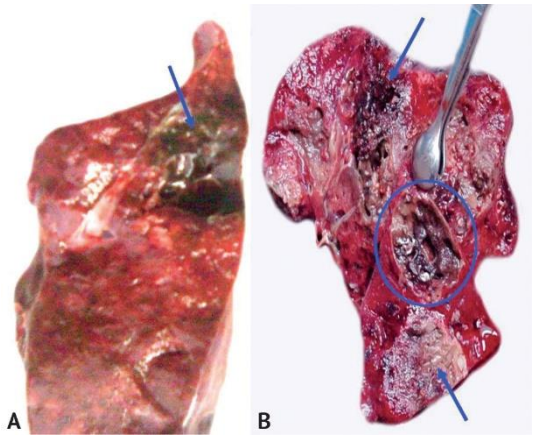

Fig. 1. A— hemorrhagic infarction of the lung (arrow); B — hemorrhagic infarction of the lung (arrows) and hemorrhagic infarction with sequestration of necrotic masses and the formation of a destructive cavity (round frame). Gross cross section of the lung

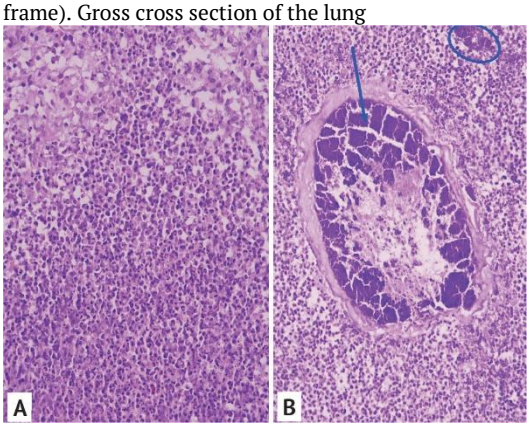

Fig. 2. A — pus focus in the lung. H&E, ×200; B — a pus focus in the lung with an accumulation of microorganisms (round frame), a blood vessel with a bacterial embolus (arrow). H&E, ×100

In the area of hemorrhagic lung infarction, the interalveolar septa are destroyed, only their outlines can be microscopically determined, cell nuclei and boundaries between cells are absent, there are hemolyzed and non-hemolyzed erythrocytes in the lumen of the alveoli. Thromboembolic occlusive masses with leukocyte infiltration and/or microbial emboli are visible in the lumen of the blood vessel (Fig. 3).

During destruction cavity formation in a hemorrhagic infarction, the inner layer is represented by necrotic masses with hemolyzed and non-hemolyzed erythrocytes, accumulations of microbial flora can be detected, the outer layer is the lung tissue with exudative changes (Fig. 4).

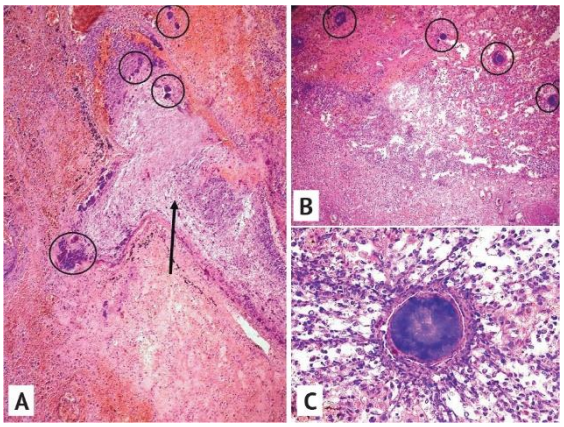

Fig. 3. A — hemorrhagic infarction of the lung, blood vessel with an infected thromboembolus (arrow); accumulation of microorganisms in the vessel and in the area of pulmonary infarction (round frame). H&E, ×100; B — hemorrhagic pulmonary infarction with multiple bacterial emboli (round frames). H&E, ×100; C — bacterial embolus in the lung. H&E, ×200

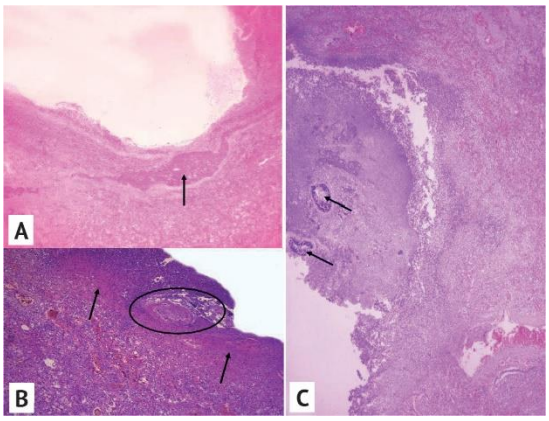

Fig. 4. A — a forming destruction cavity in hemorrhagic pulmonary infarction (blood clot in vessel is indicated by the arrow). H&E, ×40; B — the wall of forming abscess in the area of hemorrhagic pulmonary infarction (blood clot in vessel circled in oval frame; areas of hemorrhagic infarction indicated by arrows)/ H&E, ×100; C — accumulation of bacterial flora in the necrotic mass of the abscess wall. H&E, ×100

Clinically, SPE is manifested by non-specific respiratory symptoms: cough with sputum in 17.5-58.8% of patients, shortness of breath in 22.3-48.2% of patients, pleuritic chest pain in 10.8-48% of patients, hemoptysis in 14.3% of patients. In 15.5-51% of patients, hypoxemia is noted upon admission [2, 22]. Auscultation of the lungs also does not have specific differences from pneumonia of a different nature. The condition may be complicated by the development of respiratory distress syndrome, septic shock, empyema, pneumothorax, and pulmonary hypertension [20, 22, 23]. Not surprisingly, 80% of right-sided IE patients are hospitalized with an erroneous diagnosis of bilateral pneumonia [18, 24].

CHEST RADIOGRAPHY OF SPE IN PATIENTS WITH IE OF THE RIGHT HEART

Chest X-rays in patients with right-sided IE make it possible to visualize pathological changes characteristic for SPE, which often become the "signature line" of the disease, give reason to suspect IE and send the patient for echo and a bacteria culture test. In 50-100% of patients with SPE chest radiography reveals a typical bilateral lesion of the lungs with the presence of multiple small nodules, fuzzy rounded or oval shadows of various sizes, wedge-shaped shadows in the peripheral zones of the lungs (Fig. 5). Active IE is characterized by rapid development of new nodules and shadows of various volumes, their tendency to disintegrate with the emergence of thin-walled cavities; pleural effusion may also develop [3, 23, 25]. But domestic and foreign authors point to the low sensitivity of the method (22-40%), especially at initial stage of the disease [26, 27]. Chest CT scan is becoming more and more common practice. It allows you to identify characteristic changes already at the earliest stages of SPE, more objectively monitor the dynamics (which is important, both in terms of diagnostics - rapid dynamics is one of the SPE signs, - and in connection with a response to ongoing therapy), and diagnose possible complications [23].

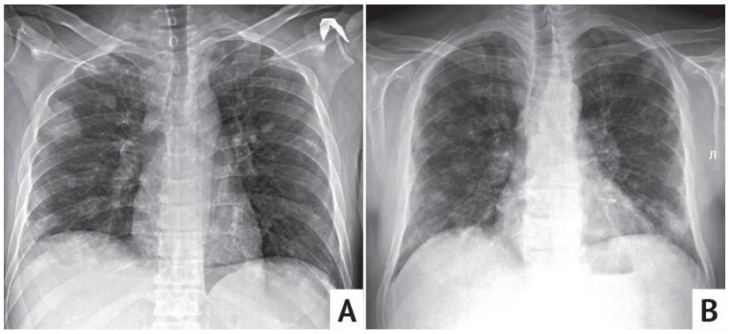

Fig. 5. Posterioanterior chest X-ray images of patients with SPE. Nodulus and round shadows across all lung fields (A), subpleural heterogeneous shadows, nodules and increased pulmonary vascularity (B). Typical ring-shaped shadows (cavities) are not detected

Patients with suspected SPE are now more likely to undergo non-contrast CT with standard scanning parameters. If the characteristic changes in the lungs are detected, it is advisable to supplement the study with intravenous contrast enhancement to exclude occlusion of large branches of the pulmonary artery (scanning into the arterial and venous phases). But unlike more common non-infectious thromboembolism, filling defects within small branches (which serve as a kind of "trap" for infected blood clots) are in practice not always detected by CT angiopulmonography due to the small caliber of the affected arteries [28]. During contrast-enhanced CT, it is also useful to assess all organs of the mediastinum, to note the ratio of the left and right parts of the heart: in case of prolonged or recurrent IE with the development of tricuspid valve (TV) insufficiency, an enlargement of the right heart occurs.

Pathological CT findings in SPE patients are diverse. The understanding of these changes is better achieved through their comparison with morphology [29]. There are 3 main types of changes that occur in patients with SPE - nodules, opacities and cavities [30]. In most cases, one patient has all these changes at the same time or, over time, they move from one pathological form to another. Thus, nodules that merge or increase in size can form opacities, and on the basis of the same nodules and opacities, destruction cavities eventually develop. SPE tends to affect both lungs, although a unilateral process can be observed at the very beginning of the disease.

The nodules in relation to the structures of the pulmonary lobule are hematogenous (chaotic - it is not possible to establish a connection of these nodules with the interstitium, some of the nodules are located along the pleura) [31], usually located on 2 sides (up to 90%) [32], for the most part of solid structure, rounded shape, with clear and even contours. According to the observations of Kuhlman J. E. et al., nodules in more than half of the cases are located in the basal sections of the lungs (61%) [33]. In the thickness of the nodules, one can observe in dynamics the appearance of destruction zones or their complete transformation into small thin-walled cavities (Fig. 6). Sometimes it can be noticed that nodules are located very close to or completely inseparable from the vascular branches - the so-called feeding vessel sign [35] which is also characteristic of hematogenous processes.

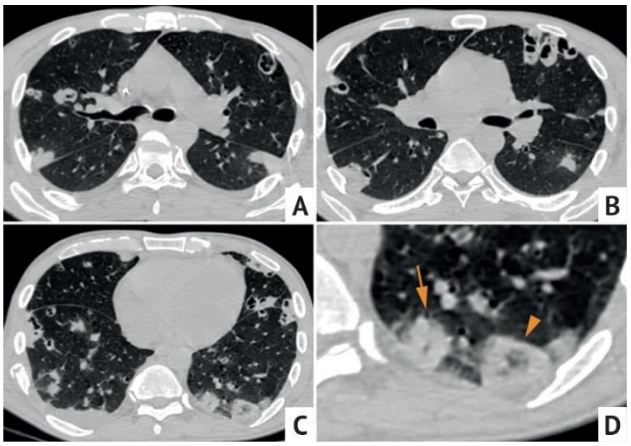

Fig. 6. Axial chest CT images (A–D) of a 35 y.o. drug user with infective endocarditis (IE) of the tricuspid valve (TV). Septic pulmonary embolism (SPE). Large number of different nodules and larger opacities (arrow) in both lungs, some of the nodules with cavitation. There are also mainly subpleurally located cavities in various stages of formation. A reversed halo sign type opacity in the lower left lobe (arrow head) is characteristic of pulmonary infarction

Opacities in most cases are also located in the subpleural zones (Fig. 7). Their shape can be triangular, semicircular or irregular [35]. The CT semiotics of consolidations is diverse: both simple consolidations without the air bronchogram sign, and areas of the halo and reverse halo signs are noted [36]. The latter sign is especially indicative - these areas are predominantly represented by infected lung infarcts (Fig. 6D, Fig. 7A). In case of halo sign, ground-glass opacity surrounds the consolidation, and reversed halo sign, also known as the atoll sign, is, on the contrary, a consolidation surrounded by an area of ground-glass opacity.

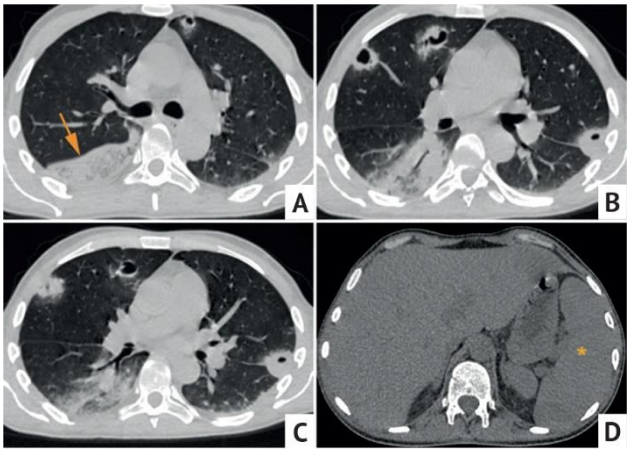

Fig. 7. Axial chest CT images (A–D) of a 34 y.o. patient with IE complicated by SPE. Small subpleural infiltrates and forming cavities. An extensive heterogeneous opacity in the right lower lobe (arrow) without the air bronchogram sign, which is more likely display a lung infarction site. Also note the enlarged spleen (*) which is also characteristic of the septic process

Almeida R.R. et al. found consolidations with reversed halo sign in 59.7% of cases, while in 46.7% of patients such consolidations were not single. Of these, 79.5% were already noted during the initial scanning, the rest in the dynamics. This sign was even more common than the halo sign (37.1%) [36].

Against the background of nodules and opacities, destruction cavities appear quite quickly - they have predominantly clear and even contours, well-defined inner and outer edges, their wall is closer by definition to elastic cavities - it has a small thickness, and some of the cavities due to their thin wall may even resemble cysts (although they are not truly ones) (Fig. 8) [37]. According to modern data, various kinds of cavities are found in the lungs of 91.9% SPE patients [36]. In some cases, there is a bay-like contour of the cavities and the presence of contents with a horizontal fluid level in their lumen; a connection with the bronchus can also be traced. Such close to regular shape of the cavities is explained by the traction ability of the lungs and their elastic properties

[38]. It is these cavities from 2 sides of the lungs that are quite pathognomonic for SPE and their diagnosis is especially specific on radiography (which can hardly be said about nodules and opacities).

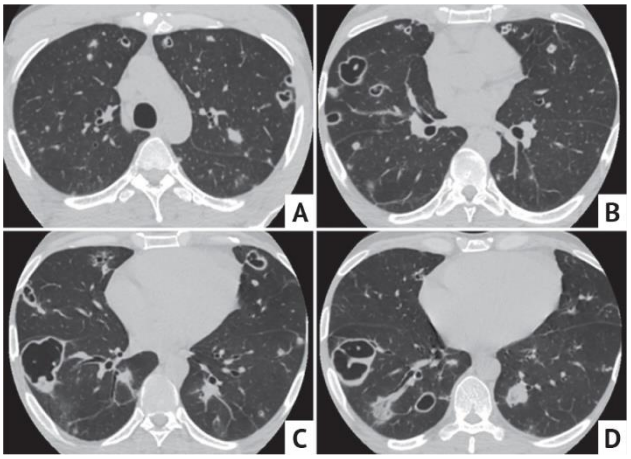

Fig. 8. Axial chest CT images (A–D) of a 38 y.o. drug user with IE of the TV. Typical SPE. Thin-walled and different sized cavities in both lungs without pus and other pathological contents, and without infiltration around the cavities

Nodules, opacities, and cavities can be located not only subpleurally, but also perivascularly, i.e. along the large pulmonary vessels, which also reflects their hematogenous nature. But this observation applies to a lesser extent to opacities of the reversed halo type because they mostly display lung infarcts having a typical subpleural position.

Intrathoracic lymph node enlargement is an additional nonspecific symptom of SPE. It occurs in 24.4-27.3% of cases, is reactive and never takes the form of widespread lymphadenopathy [39]. Pleural effusion may be detected in SPE, especially in the presence of subpleural cavities or infarcts, which will determine the nature of the effusion (exudate, empyema, hemorrhagic fluid). In some cases, the incidence of pleural effusion reaches 64.3%, second only to focal changes [40]. A summary of the main CT symptoms of SPE is presented in Table 1.

Table 1

Basic CT patterns of SPE

CT sign	Feature
Nodules	– Chaotic – Subpleural and perivascular – Size from 5.0 mm – Transformation with destruction – Feeding vessel sign
Opacities	– Subpleural and perivascular – Wedge-shaped or irregular shape – Outlines are often quite clear – Halo or reversed halo sign – Destruction in the thickness
Destruction cavities	– Subpleural and perivascular – Multiple, mostly thin-walled – Possible contents with horizontal fluid level, communication with the bronchi
Pleura changes	– Reactive effusion or empyema (thickening of the pulmonary pleurae, contrast enhancement) – Pneumothorax (due to rupture of cavities) or its combination with pleural effusion
Lymph nodes	– Enlargement of single ones (reactive type) – No structural changes (no calcifications, destruction, pathological contrast enhancement)
General signs	– In the vast majority of cases – bilateral process and the simultaneous presence of all the above signs – Possible filling defects in the branches of the pulmonary artery during contrast – Transformation of some pathological structures into others over time – Rapid dynamics of progression with the formation of destruction cavities (without therapy) – Healing usually leads to areas of fibrosis, less often leaves no trace

Despite the apparent complexity and polymorphism of manifestations, the CT-semiotics of SPE is quite stereotyped; understanding its pathogenesis, it is easier to characterize the existing elements of the picture, especially if the assessment is carried out in dynamics.

The immediate complications of SPE include the progression of destruction cavities with their possible fusion and the formation of large abscesses, the occurrence of massive pneumonic infiltration in the lungs, the formation of fistulas, incl. with the pleura, and the development of empyema, pneumothorax, and acute respiratory distress syndrome (ARDS) [30]. Pneumothorax as a complication of SPE can be unilateral or bilateral [41]. As in other cases with lung cavities, it develops if the latter are located close to the pleura, their rupture and the formation of communication between them and the pleural cavity, through which air enters (Fig. 9).

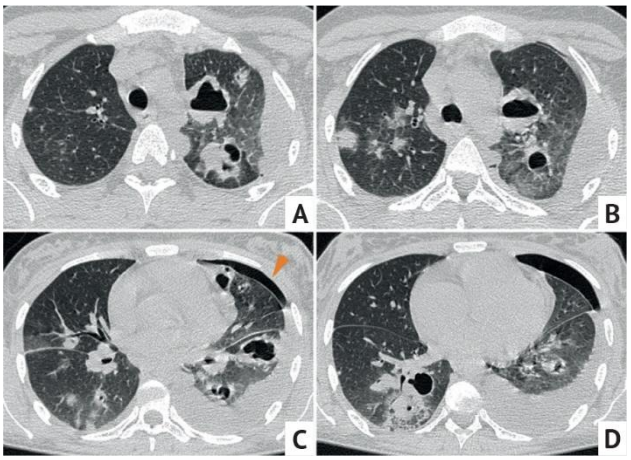

Fig. 9. Axial chest CT images (A–D) of a 23 y.o. patient with sepsis (IE of the TV, pelvic abscess, SPE), HIV, hepatitis C. Lungs infiltrates and cavities, part of the cavities (in the upper left lobe) — with a horizontal fluid level. Acute chest pain on the left was the main reason for hospitalization, which was associated with air (arrow) and fluid contents in the pleural cavity (hydropneumothorax). The probable cause is a rupture of the subpleurally located cavities

ARDS usually develops in conjunction with an uncontrolled septic process. The morphological picture of diffuse alveolar damage in SPE on CT looks like the appearance against the background of the above described characteristic changes of confluent foci and ground-glass areas and consolidations on 2 sides, which are more inclined towards the nuclear parts of the lungs or located diffusely; a combination of ground-glass opacification with a thickening of the intralobular interstitium of the cobblestone pavement type is possible (Fig. 10).

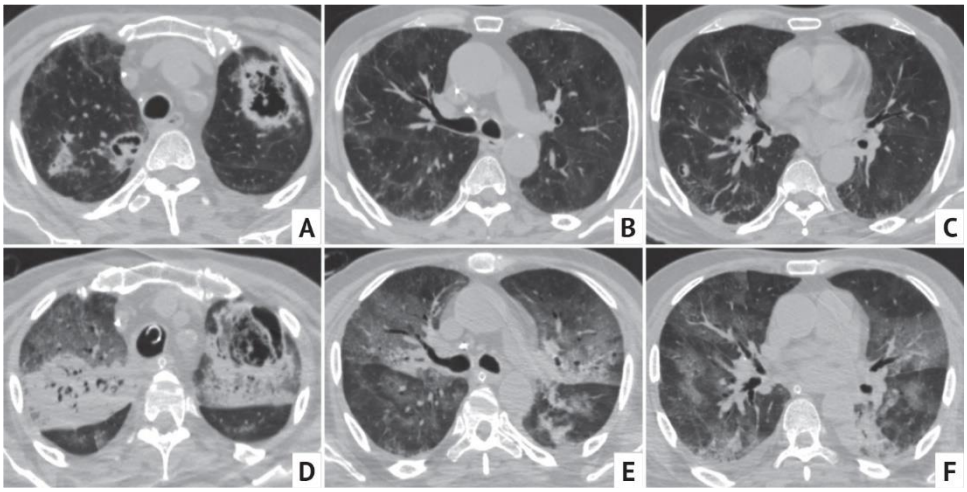

Fig. 10. Axial chest CT images of a 68 y.o patient with poorly-controlled diabetes mellitus, after COVID-19 infection from 13.09.2020 (A–C) and from 21.09.2020 (D–F) at the corresponding levels. Embolic lung cavities (IE was diagnosed), negative dynamics. ARDS as a result of Klebsiella sepsis (multidrug resistant Klebsiella pneumoniae) — appearance of extensive ground-glass opacity (GGO) and consolidations

DIFFERENTIAL DIAGNOSIS OF SPE VERSUS THAT OF OTHER DISEASES ACCORDING TO DIAGNOSTIC RADIOLOGY

The differential diagnosis of SPE includes a number of diseases, where the formation of nodules with destruction cavities predominates [34].

The corresponding differential diagnostic criteria are presented by us in Table 2.

Table 2

Differential diagnosis of SPE according to chest CT patterns

Nosology	Basic CT features
Pulmonary tuberculosis	– Cavities closer to irregular shape, bay-shaped internal contours, thicker walls – The number of cavities is usually smaller, they gravitate towards the upper sections – Nodules of bronchogenic dissemination (!) – In disseminated forms – hematogenous foci, often irregular in shape, more closely-grouped – Calcifications and bronchiectasis in the lungs, calcification in intrathoracic lymph nodes – Relatively slow pace of change
Fungal infection	– Slow development of cavities, they are more often single – Monod sign –Bronchiectasis, bronchogenic foci (tree-in-bud sign) – Halo sign in patients with angioinvasive forms
Granulomatosis with polyangiitis	– Subpleural opacities (including with halo or reversed halo signs) – Destructive formations against the background of opacities, thin-walled cavities – Hematogenous foci, rounded formations – Thickening of the walls of the bronchi and trachea (!) – Slow development of changes in dynamics
Rheumatoid nodules in the lungs	– A few chaotic nodules with clear contours – Possible destructive formations in the nodules – Opacities and cavities are not typical – Slow dynamics of the appearance of nodules – May be associated with interstitial manifestations (UIP/NSIP)
Cavitating pulmonary metastases	– Nodules and destructive formations are usually small or medium sized, wall thickness varies – Combination with "classic" solid metastases – Opacities and large–diameter cavities are not typical – Slow dynamics in the absence of chemotherapy

Notes: UIP — usual interstitial pneumonia; NSIP — nonspecific interstitial pneumonia

An important part of the differential diagnosis of focal lesions is the determination of the nature of the lesions. SPE is a hematogenous process, therefore, hematogenous nodules are found, both opacities and cavities also tend to be perivascular. The presence of bronchogenic lesions usually rules out SPE.

For differential diagnosis, it is principal to conduct CT in follow-up images - SPE is characterized by a fairly rapid course of the process - the transformation of existing nodules and opacities into cavities within 2-7 days, the appearance of new pathological changes in previously intact areas of the lungs (which reflects the recurrence of embolism, especially frequent in large valvular vegetations without specific therapy) (Fig. 11) [37]. This helps to differentiate SPE from such nosologies as fungal infection in the lungs, when cavities form more slowly, usually there are fewer of them, fungal bodies are detected in the cavities in the form of Monod sign - it is multiple mycetomas that are most similar to SPE according to the CT picture (Fig. 12). But the presence of fungal bodies is not a prerequisite for cavities in aspergillosis, which makes interpretation difficult. Not all forms of aspergillosis can be similar to SPE in CT picture – differentiation requires aspergilloma, as well as chronic cavitary forms [42].

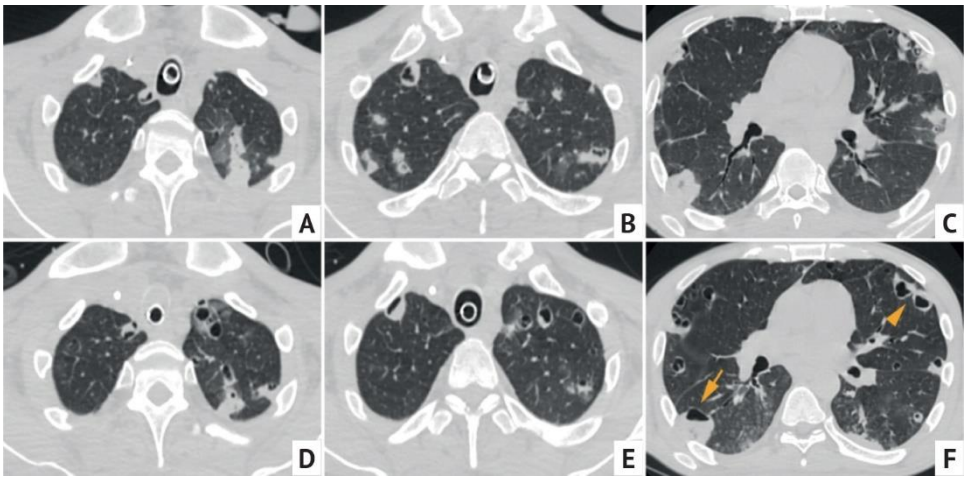

Fig. 11. Axial chest CT images of a 35 y.o patient from 19.08.2018 (A–C) and from 24.08.2018 (D–F) at the corresponding levels. SPE as a complication of IE of the TV. New lungs nodules in follow-up images are noted, as well as the formation of cavities against the background of opacities (arrows)

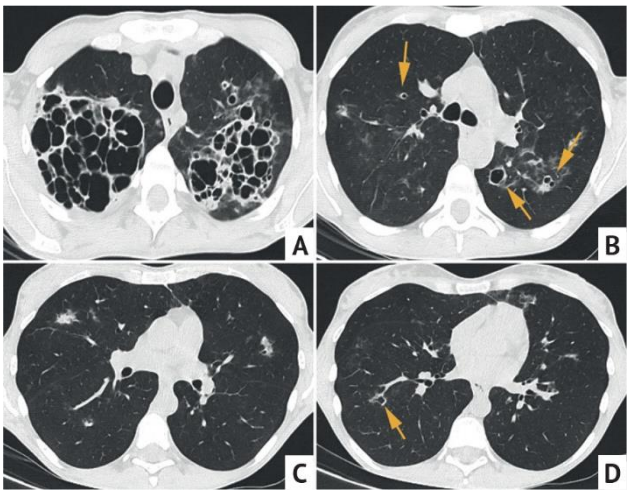

Fig. 12. Axial chest CT images of 42 y.o patient (A–D), HIV, candidasis of the esophagus. In addition to large multi-chamber cavities in the upper lobes (not typical for SPE), in other parts of the lungs, small thin-walled cavities with clear contours (arrows), small infiltrates are determined. Growth of Candide, Aspergillus fungi in the lavage fluid during bronchoscopy

The most relevant is the differentiation of SPE from pulmonary tuberculosis - subacute hematogenous disseminated tuberculosis, as well as its severe forms. In tuberculosis, a different type of cavities is found with thicker walls (often irregularly shaped without contents inside, with bay-shaped internal contours, fibrous transformation is observed around the cavity during a long course, liquid contents are rarely present in the cavities), the presence of calcifications and bronchiectasis, nodules of bronchogenic dissemination are typical, which are not found in SPE, a much slower dynamics of changes (Fig. 13, 14). One should not forget nontuberculous mycobacterial (NTM) lung disease, because cavitary forms and focal lesions may resemble the CT picture of SPE [43].

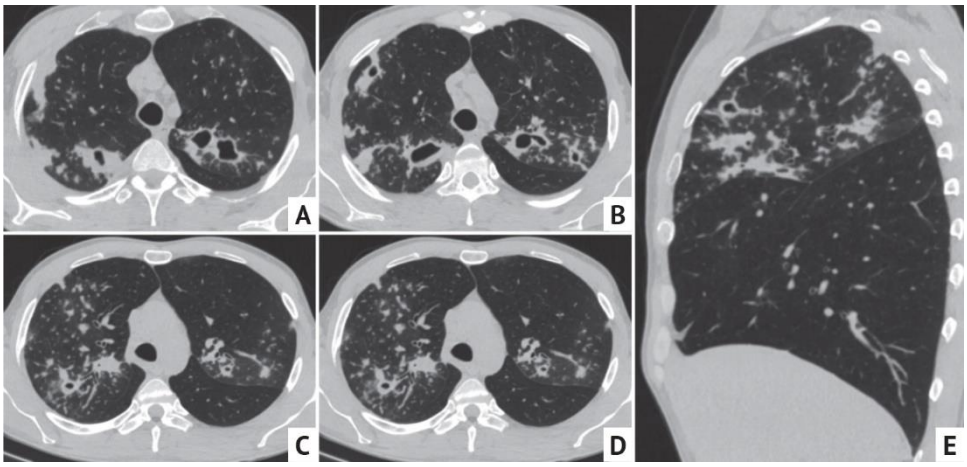

Fig. 13. Axial (A–D) and sagittal (E) chest CT images of 40 y.o patient with pulmonary tuberculosis. Irregular shaped cavities (caverns) with relatively thin walls in the upper lung lobes against the background of many hematogenic and bronchogenic nodules, infiltrates

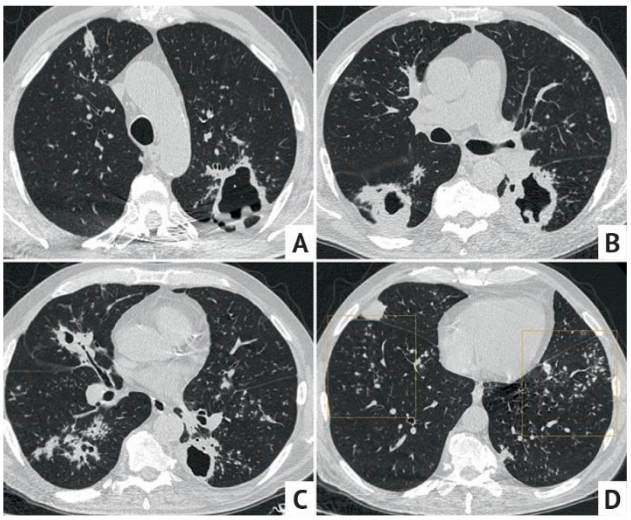

Fig. 14. Axial chest CT images of 44 y.o patient with pulmonary tuberculosis. In the upper lobe, as well as in S6 on the left, there are irregular caverns with bay-shaped contours without content, walls is quite thick, there are no fibrosis around. There are nodules of bronchogenic dissemination (boxes) in all parts of the lungs (A–D)

Multiple bilateral subpleural/peribronchial infiltrates are observed in granulomatosis with polyangiitis (in almost 70% of cases), in the thickness of these opacities, aseptic destructive formations may occur without contents in the lumen or thin-walled cavities, and in 46.7% of patients there is segmental and subsegmental bronchial wall thickening [44]. Similar to SPE, nodules (more often of the hematogenous type) and larger formations, halo and reversed halo sign opacities are found in the lungs (Fig. 15). Due to the great similarity of radiation signs, differential diagnosis in this case should mainly be based on the nature of the clinical course and concomitant manifestations (hemorrhagic rhinitis, sinusitis, kidney damage), as well as the dynamics of the process [45]. One of the important differential CT signs may be circular tracheal wall thickening, incl. its membranous part, which is not found in SPE [46].

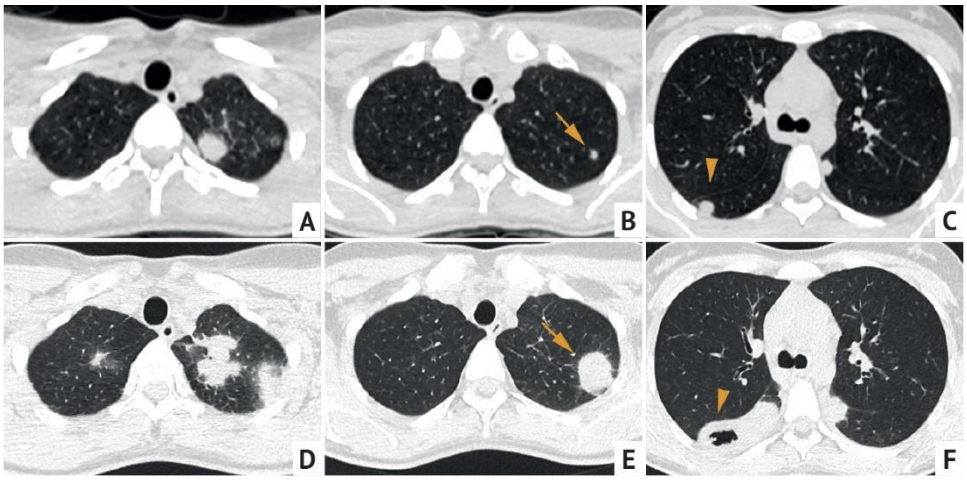

Fig. 15. Axial chest CT images of 30 y.o patient from 29.11.2018 (A–C) and 19.12.2019 (D–F) at the corresponding levels. Granulomatosis with polyangiitis (histologically verified). Nodular rounded tumor-like formations in both lungs with slow progression — an increase in size (arrow), the appearance of destruction in place of one of the nodes (arrow head)

Necrotic (rheumatoid) lung nodules are found in systemic connective tissue diseases (for example, in rheumatoid arthritis), but large cavities and infiltrates almost never form during this process. A combination of focal changes with an interstitial lesion of the type of usual (UIP) or nonspecific interstitial pneumonia (NSIP) is possible, which simplifies the interpretation of the CT picture in first-time patients. The asymptomatic course prevails – this, on the contrary, makes it difficult to establishing diagnosis in patients who are not observed by a rheumatologist for the underlying disease [45, 47].

Cavities of various sizes, often thin walled, can be found in case of cavitating pulmonary metastases. The occurrence of cavities in metastases is associated with necrosis in their thickness (due to circulatory disorders), mucoid degeneration of the metastasis center, or a valve mechanism in case of connection with the bronchi. Decays can also be formed under the action of chemotherapy [48]. They may be combined with characteristic hematogenous nodules with torose and radial contours (Fig. 16). According to CT data, cavitating metastases account for 8.3% of all types of metastases. More often, such metastases occur in adenocarcinomas of the breast, gastrointestinal tract (colon predominates), sarcomas, squamous cell carcinoma of the head and neck (for example, nasopharynx), cervix, etc. [49]. Unlike SPE, infiltrates, large cavities are not typical for metastatic lesions, and the dynamics of changes is much slower. Clinical manifestations of these changes may be absent for a long time.

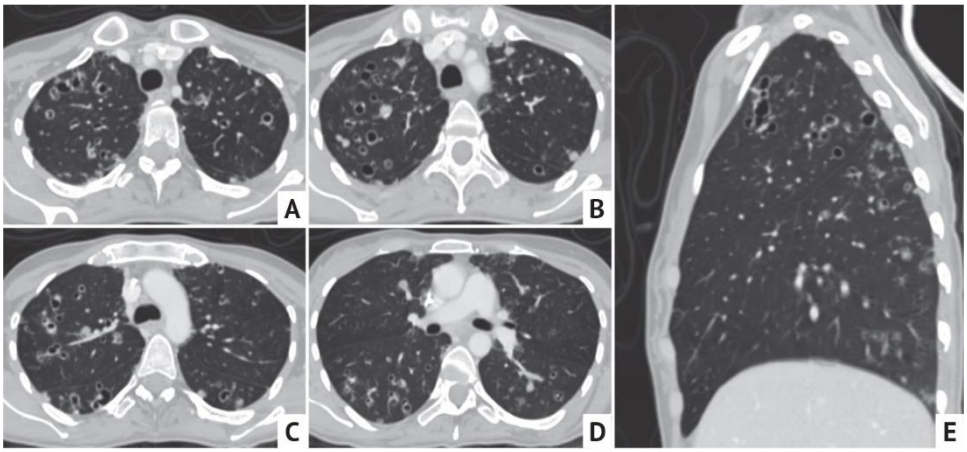

Fig. 16. Axial (A–D) and sagittal (E) chest CT images of 35 y.o patient with ovary sarcoma. Cavitating pulmonary metastases. In both lungs, more in the upper parts — multiple small thin-walled cavities and nodules with cavitation of a rounded shape with clear contours. Infiltrates and large cavities are absent

To compare the appearance of typical cavities and destructive formations in the lungs according to CT data for the most common nosologies, see Fig. 17.

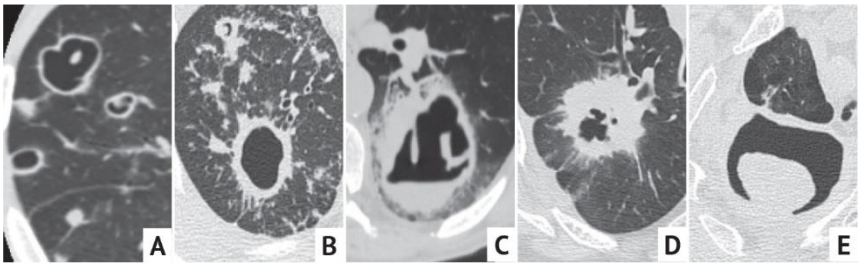

Fig. 17. Comparison of typical cavities and destructions in various diseases. A — septic pulmonary embolism, B — tuberculosis, C — acute abscess, D — cancer with decay, E — aspergilloma (mycetoma)

DIFFERENTIAL DIAGNOSIS OF SPE AND VIRAL LUNG INJURY DUE TO COVID-19

Since the beginning of the pandemic caused by the nSARS-CoV2 virus, the issue of differential diagnosis of these two diseases seems to be topical. It is not uncommon for patients with SPE to be admitted to hospitals for COVID-19 treatment during their initial hospitalization due to similar clinical presentation (fever, cough, dyspnea). In most cases, CT helps to carry out differential diagnostics already at the level of the admission department, with a high probability allowing to exclude or confirm SPE due to different CT semiotics - in case of viral damage, nodules, formation of cavities, pleural effusion are not typical. In the overwhelming majority of patients, areas of ground glass opacification located subpleurally and along the course of the vascular bundles in combination with reticular striations or without them prevail [50-52]. The symptom of ground glass opacification in itself is not typical for SPE. At the same time, subpleural consolidations are formed in a number of patients at the site of ground glass opacification only in dynamics and are represented by areas of organizing pneumonia or hemorrhages; according to CT data, they have a different shape and are combined with bundles, perilobular consolidations [53]. The reverse halo sign is rare, but it can also be observed in the acute period of COVID-19 course, however, consolidations look different (Fig. 18).

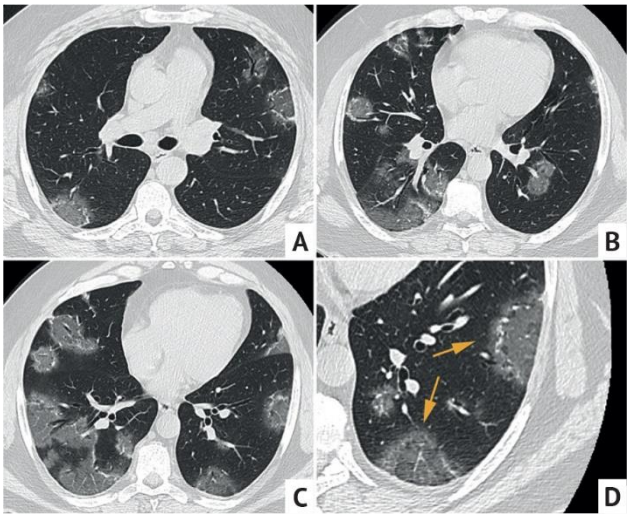

Fig. 18. Axial chest CT images of 41 y.o patient (A–C) with enlarged fragment of left lung (D). COVID-associated lung damage. Opacities like "reverse halo" sign (arrows) without cavitating in both lungs. The type of current opacities differs from those in lung infarction — there is no typical reticulation on the background of GGO, a less pronounced rim of consolidation

Difficulties can arise when viral damage to the lungs is combined with areas of infarction against the background of PE [54]. However, in contrast to SPE, infarctions in PE are rarely multiple, decays against their background have an irregular shape (characteristic cavities are not formed) (Fig. 19). Disintegrations in infarcts against the background of PE develop relatively slowly, and SPE is characterized by the rapid destruction formation.

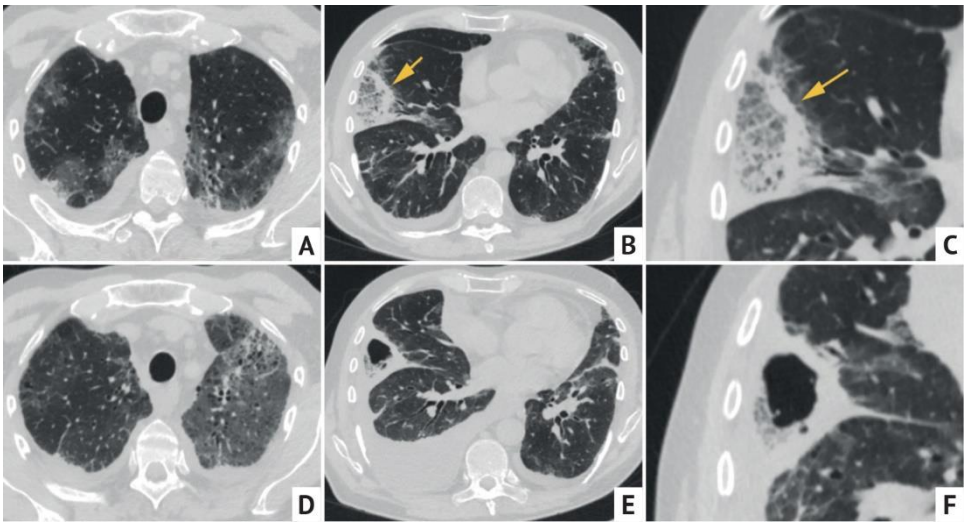

Fig.19. Axial chest CT images of a 65 y.o patient with COVID-19 and pulmonary embolism (with infarction in the right middle lobe) from 15.10.2020 (A–C) and from 22.10.2020 (D–F) at the corresponding levels. In the middle right lobe, a reversed halo sign type opacity (arrows) is clearly visible. A week after the initial study, lung cavitation appeared in the infarction site, and pleural effusion increased. Nodules and other cavities are not detected

DIAGNOSIS OF RIGHT-SIDED INFECTIVE ENDOCARDITIS IN PATIENTS WITH SPE SYNDROME

Although right-sided IE is responsible for about a quarter of SPE cases, infected clots can also travel to the right heart and further on into the pulmonary artery system from other sources. It is not infrequent that the source of septic emboli is suppurative processes in the skin and soft tissues, less often - septic thrombophlebitis of the internal jugular vein in case of spread of infection from the oral cavity and pharynx (Lemierre's syndrome), oral abscesses, peripheral abscesses, osteomyelitis, infected thrombi of peripheral veins and vena cava [41, 55]. The diagnosis of right-sided IE in this clinical setting is most likely found in intravenous drug users or in the presence of predisposing heart disease. Therefore, it is advisable to indicate in the protocol of radiological examinations, the presence of valve prostheses and wires of the pacemaker electrodes, as predisposing to IE [56], as well as the changes detected at the scanning level, for example, characteristic of IE enlargement of the spleen [33]. SPE is one of the minor diagnostic signs of right-sided IE, but to verify IE in the right heart, all patients with SPE need to undergo transthoracic echo (or transesophageal echo in the presence of a permanent pacemaker) and a bacteria culture test within 24 hours [17].

CONCLUSION

IE of the right heart is characterized by a “lung mask” caused by SPE, which occurs due to recurrent embolism of the pulmonary arteries by infected fragments of vegetation. Although SPE has no specific clinical features, multiple rapidly changing pulmonary lesions and abscessed infiltrates raise the suspicion of SPE and right-sided IE. In most cases, the diagnosis of SPE is based on the findings of a chest CT scan. Therefore, this study, along with echocardiography and a bacteria culture test, is mandatory in all cases of suspected IE of the right heart, as well as in all patients with risk factors for right-sided IE (intravenous drug addiction, permanent pacemaker, hemodialysis, etc.) with fever of unspecified origin persisting more than a week and non-specific respiratory symptoms.

REFERENCES

1. Lee MR, Chang SA, Choi SH, Lee GY, Kim EK, Peck KR, et al. Clinical Features of Right-Sided Infective Endocarditis Occurring in Non-Drug. *Users J Korean Med Sci*. 2014;29(6):776–781. PMID: 24932077 https://doi.org/10.3346/jkms.2014.29.6.776
2. Yuan SM. Right-sided infective endocarditis: recent epidemiologic changes. *Int J Clin Exp Med.* 2014;7(1):199–218. PMID: 24482708 eCollection 2014.
3. Chipigina NS, Shostak NA, Vinogradova TL, Malysheva AM. Infective Endocarditis in Intravenous Drug Users. *Bulletin of RSMU*. 2009;(7):97–101. (in Russ.)
4. Cresti A, Baratta P, De Sensi F, D'Aiello I, Costoli A, Limbruno U. Frequency and Clinical Significance of Right Atrial Embryonic Remnants Involvement in Infective Endocarditis. *J Heart Valve Dis*. 2017;26(6):700–707. PMID: 30207121
5. Song G, Zhang J, Zhang X, Yang H, Huang W, Du M, et al. Right-sided infective endocarditis with coronary sinus vegetation. *BMC Cardiovasc Disord*. 2018;18(1):111. PMID: 29866073 https://doi.org/10.1186/s12872-018-0845-x
6. Rudasill SE, Sanaiha Y, Mardock AL, Khoury H, Xing H, Antonios JW, et al. Clinical Outcomes of Infective Endocarditis in Injection Drug Users. *J Am Coll Cardiol.* 2019;73(5):559–570. PMID: 30732709 https://doi.org/10.1016/j.jacc.2018.10.082
7. Chipigina NS, Karpova NYu, Anichkov DA, Kondratieva TB. Infectious Endocarditis in the Elderly – Comparative Study of Clinical Features, Course and Outcomes. *Rational Pharmacotherapy in Cardiology*. 2020;16(2):166–174. https://doi.org/10.20996/1819-6446-2020-03-02
8. Moiseev VS, Kobalava ZD, Pisaryuk AS, Milto AS, Kotova EO, Karaulova YL, et al. Infective Endocarditis in Moscow General Hospital: Clinical Characteristics and Outcomes (Single-Center 7 Years' Experience). *Kardiologiia*. 2018;58(12):66–75. (in Russ.) https://doi.org/10.18087/cardio.2018.12.10192
9. Frontera JA, Gradon JD. Right-side endocarditis in injection drug users: review of proposed mechanisms of pathogenesis. *Clin Infect Dis*. 2000;30(2):374–379. PMID: 10671344 https://doi.org/10.1086/313664
10. Revilla A, López J, Villacorta E, Gomez I, Sevilla T, Angel del Pozo M, et al. Isolated right-sided valvular endocarditis in non-intravenous drug users. *Rev Esp Cardiol*. 2008;61(12):1253–1259. PMID: 19080963 https://doi.org/10.1016/s1885-5857(09)60052-9
11. Asgeirsson H, Thalme A, Weiland O. Low mortality but increasing incidence of Staphylococcus aureus endocarditis in people who inject drugs: Experience from a Swedish referral hospital. *Medicine (Baltimore)*. 2019;95(49):e5617. PMID: 27930590 https://doi.org/10.1097/MD.0000000000005617
12. Chipigina NS, Karpova NYu, Tulinov MM, Golovko EV, Goloukhova LM, Kornienko VS, et al. Primary infective endocarditis with isolated involvement of the pulmonary valve not associated with drug addiction. *The Clinician*. 2019;13(1–2):65–71. (in Russ.) https://doi.org/10.17650/1818-8338-2019-13-1-2-65-71
13. Hussain ST, Shrestha NK, Witten J, Gordon SM, Houghtaling PL, Tingleff J, et al. Rarity of invasiveness in right-sided infective endocarditis. *J Thorac Cardiovasc Surg.* 2018;155(1):54–61. PMID: 28951083 https://doi.org/10.1016/j.jtcvs.2017.07.068
14. Blomström-Lundqvist C, Traykov V, Erba PA, Burri H, Nielsen JC, Bongiorni MG, et al. ESC Scientific Document Group. European Heart Rhythm Association (EHRA) international consensus document on how to prevent, diagnose, and treat cardiac implantable electronic device infections-endorsed by the Heart Rhythm Society (HRS), the Asia Pacific Heart Rhythm Society (APHRS), the Latin American Heart Rhythm Society (LAHRS), International Society for Cardiovascular Infectious Diseases (ISCVID) and the European Society of Clinical Microbiology and Infectious Diseases (ESCMID) in collaboration with the European Association for Cardio-Thoracic Surgery (EACTS). *Europace*. 2020;22(4):515–549. PMID: 31702000 https://doi.org/10.1093/europace/euz246
15. Demko IV, Pelinovskaya LI, Mankhayeva MV, Ishchenko OP, Mosina VA, Kraposhina AYu, et al. Features of infective endocarditis in injection drug users. *Russian Journal of Cardiology.* 2019;(6):97–102. (in Russ.) https://doi.org/10.15829/1560-4071-2019-6-97-102
16. Hatori K, Ohki S, Obayashi T, Yasuhara K, Hirai H, Miki T. Surgical case of isolated pulmonary valve endocarditis in a patient without predisposing factors. *Gen Thorac Cardiovasc Surg.* 2018;66(4):235–238. PMID: 28589481 https://doi.org/10.1007/s11748-017-0788-7
17. Habib G, Lancellotti P, Antunes MJ, Bongiorni MG, Casalta J-P, Del Zotti F, et al.; ESC Scientific Document Group. 2015 ESC Guidelines for the management of infective endocarditis: The Task Force for the Management of Infective Endocarditis of the European Society of Cardiology (ESC). Endorsed by: European Association for Cardio-Thoracic Surgery (EACTS), the European Association of Nuclear Medicine (EANM). *Eur Heart J*. 2015;36(44):3075–3128. PMID: 26320109 https://doi.org/10.1093/eurheartj/ehv319
18. Chipigina NS, Karpova NYu, Belova MV, Savilov NP. Infective endocarditis: diagnostic difficulties. *The Clinician*. 2020;14(1–2):82–90. (in Russ.) https://doi.org/10.17650/1818-8338-2020-14-1-2-82-90
19. Stolbova MV, Liscova UV, Artemova NE, Saifutdinov RI, Bugrova OV. Features of an Infectious Endocarditis in Injection «Salt» Addicts. *The Russian Archives of Internal Medicine*. 2017;7(4):267–270. (in Russ.) https://doi.org/10.20514/2226-6704-2017-7-4-267-270
20. Swaminath D, Yaqub Y, Narayanan R, Paone R, Nugent K, Arvandi A. Isolated Pulmonary Valve Endocarditis Complicated with Septic Emboli to the Lung Causing Pneumothorax, Pneumonia, and Sepsis in an Intravenous Drug Abuser. *J Investig Med High Impact Case Rep*. 2013;1(4):2324709613514566. PMID: 26425590 https://doi.org/10.1177/2324709613514566 eCollection 2013 Oct-Dec.
21. Chahoud J, Sharif Yakan A, Saad H, Kanj SS. Right-Sided Infective Endocarditis and Pulmonary Infiltrates: An Update. *Cardiol Rev*. 2016;24(5):230–237. PMID: 26501991 https://doi.org/10.1097/CRD.0000000000000095
22. Ye R, Zhao L, Wang C, Wu X, Yan H. Clinical characteristics of septic pulmonary embolism in adults: a systematic review. *Respir Med.* 2014;108(1):1–8. PMID: 24183289 https://doi.org/10.1016/j.rmed.2013.10.012
23. Shmueli H, Thomas F, Flint N, Setia G, Janjic A, Siegel R. Right-Sided Infective Endocarditis 2020: Challenges and Updates in Diagnosis and Treatment. *J Am Heart Assoc*. 2020;9(15):e017293. PMID: 32700630 https://doi.org/10.1161/JAHA.120.017293
24. Bamford P, Soni R, Bassin L, Kull A. Delayed diagnosis of right-sided valve endocarditis causing recurrent pulmonary abscesses: a case report. *J Med Case Rep*. 2019;13(1):97. PMID: 30999926 https://doi.org/10.1186/s13256-019-2034-7
25. Zuo LE, Guo S. Septic pulmonary embolism in intravenous drug users. *Zhonghua Jie He He Hu Xi Za Zhi*. 2007;30(8):569–572. PMID: 17988547
26. Koroleva IM, Sokolina IA, Lemeshko ZA, Ganina SS, Kokina NI. Diagnostic Imaging of Septic Lungs Emboli With Patients With Purulent Diseases of Maxillofacial Region. *Medical Visualization*. 2007;(1):69–73. (in Russ.).
27. Mendez-Echevarria A, Coronado-Poggio M, Baquero-Artigao F, Rosal TD, Rodado-Marina S, Calvo C, et al. Septic pulmonary emboli detected by 18F-FDG PET/CT in children with S. aureus catheter-related bacteremia. *Infection*. 2017;45(5):691–696. PMID: 28243995 https://doi.org/10.1007/s15010-017-0992-5
28. Chou DW, Wu SL, Chung KM, Han SC. Septic pulmonary embolism caused by a Klebsiella pneumoniae liver abscess: clinical characteristics, imaging findings, and clinical courses. *Clinics*. 2015;70(6):400–407. PMID: 26106957 https://doi.org/10.6061/clinics/2015(06)03

29. Huang RM, Naidich DP, Lubat E, Schinella R, Garay SM, McCauley D. Septic pulmonary emboli: CT-radiographic correlation. *AJR Am J Roentgenol*. 1989;153(1):41–45. PMID: 2735296 https://doi.org/10.2214/ajr.153.1.41
30. Vinokurov AS, Yudin AL, Belenkaya OI. CT-signs of septic pulmonary embolism and it's complications. *Medical Visualization*. 2018;22(6):23–32. (in Russ.) https://doi.org/10.24835/1607-0763-2018-6-23-32
31. Tyurin IE. Differential Diagnosis of Focal Changes on Computed Tomography. *Journal of Radiology and Nuclear Medicine*. 2013;(6):44–50.
32. Ojeda Gómez JSA, Carrillo Bayona JA, Morales Cifuentes LC. Septic pulmonary embolism secondary to Klebsiella pneumoniae epididymitis: Case report and Literature review. *Case Rep Radiol*. 2019;2019:5395090. PMID: 31016062 https://doi.org/10.1155/2019/5395090 eCollection 2019.
33. Kuhlman JE, Fishman EK, Teigen C. Pulmonary septic emboli: diagnosis with CT. *Radiology*. 1990;174(1):211–213. PMID: 2294550 https://doi.org/10.1148/radiology.174.1.2294550
34. Inchaustegui CA, Wang KY, Teniola O, Rosen VL. Large septic pulmonary embolus complicating streptococcus mutans pulmonary valve endocarditis. *Radiology Case*. 2018;12(2):18–27. PMID: 29875987 https://doi.org/10.3941/jrcr.vl2i2.3240
35. Iwasaki Y, Nagata K, Masaki N, Natuhara A, Harada H, Kubota Y, et al. Spiral CT findings in septic pulmonary emboli. *EJR Eur J Radiol*. 2001;37(3):190–194. PMID: 11274848 https://doi.org/10.1016/s0720-048x(00)00254-0
36. Almeida RR, Marchiori E, Flores EJ. Frequency and reliability of the reversed halo sign in patients with septic pulmonary embolism due to IV substance use disorder. *AJR Am J Roentgenol*. 2020;214(1):59–67. PMID: 31670590 https://doi.org/10.2214/AJR.19.21659
37. Vlasov PV, Karmazanovsky GG, Sheikh ZhV, Vilyavin MYu. B Cysts фnd Cystic Like Lungs Lesions. *Medical Visualization*. 2005;(1):82–94. (in Russ.).
38. Bogatov AI, Mustafin DG. *Oslozhnennaya stafilokokkovaya pnevmoniya u vzroslykh*. Moscow: Meditsina Publ.;1984.
39. Oh GH, Cha SI, Shin KM, Lim JK, Kim HJ, Yoo SS, et al. Risk factors for mortality in patients with septic pulmonary embolism. *J Infect Chemoter*. 2016;22(8):553–558. PMID: 27346380 https://doi.org/10.106/j.jiac.2016.05.008
40. Jiang J, Liang QL, Liu LH, Cai SQ, Du ZY, Kong JL, et al. Septic pulmonary embolism in China: clinical features and analysis of prognostic factors for mortality in 98 cases. *BMC Infectious Diseases.* 2019;19(1):1082. PMID: 31881849 https://doi.org/10.1186/s12879-019-4672-1
41. Galili Y, Lytle M, Carlan S, Madruga M. Bilateral pneumothoraces: a rare complication of septic pulmonary emboli in intravenous drug abusers. *Am J Case Rep*. 2018;19:829–832. PMID: 30006503 https://doi.org/10.12659/AJCR.91037
42. Kosmidis C, Denning DW. The clinical spectrum of pulmonary aspergillosis. *Thorax*. 2015;70(3):270–277. PMID: 25354514 https://doi.org/10.1136/thoraxjnl-2014-206291
43. Gavrilov P, Archakova L, Anisimova A, Kolesnichenko O. Radiological semiotics mycobacteriosis of the lungs caused by M. avium in immunocompetent patients. *Medical Alliance*. 2019;(1):31–37. (in Russ.).
44. Sokolina IA, Koroleva IM. Possibilities of Computed Tomography in the Diagnosis of Primary Pulmonary Vasculitis. *Journal of Radiology and Nuclear Medicine.* 2014;(1):10–18. (in Russ.) https://doi.org/10.20862/0042-4676-2014-0-1-10-18
45. Aver'yanov AV, Lesnyak VN, Kogan EA. *Redkie zabolevaniya legkikh: diagnostika i lechenie*. Moscow: Meditsinskoe informatsionnoe agentstvo Publ.; 2016. (in Russ.).
46. Martinez F, Chung JH, Digumarthy SR, Kanne JP, Abbott GF, O Shepard JA, et al. Common and uncommon manifestation of Wegener granulomatosis at chest CT: radiologic-pathologic correlation. *RadioGraphics*. 2012;32(1):51–69. PMID: 22236893 https://doi.org/10.1148/rg/321115060
47. Ayer A, Sliesoraitis S, Valez R. Necrobiotic cavitary pulmonary nodules: a case report. *J Pulmon Resp Med*. 2012;2(4):126. https://doi.org/10.4172/2161-105X.1000126
48. Seo JB, Im JG, Goo JM, Chung MJ, Kim MY. Atypical pulmonary metastases: spectrum of radiologic findings. *RadioGraphics*. 2001;21(2):403–417. PMID: 11259704 https://doi.org/10.1148/radiographics.21.2.g01mr17403
49. Yu X, Wang P, Liang Zh. Cavitary pulmonary metastases: CT features and their correlation with the pathology of the primary malignancy. *Chinese-German J Clin Oncol*. 2004;3(1):29–33. https://doi.org/10.1007/s10330-004-0208-1
50. Vinokurov AS, Belenkaya OI, Zolotova EA, Michurina SV, Vinokurova OO, Nikiforova MV, et al. Differential diagnosis of bilateral lungs opacities in the hospital for admission of community-acquired pneumonia – not only COVID-19. *Medical Visualization*. 2020;24(2):78–95. (in Russ.) https://doi.org/10.24835/1607-0763-2020-2-78-95
51. Salehi S, Abedi A, Balakrishnan S, Gholamrezanezhad A. Coronavirus Disease 2019 (COVID-19): A Systematic Review of Imaging Findings in 919 Patients. *AJR Am J Roentgenol*. 2020;215(1):87–93. PMID: 32174129 https://doi.org/10.2214/AJR.20.23034
52. Revzin MV, Raza S, Warshawsky R, D'Agostino C, Srivastava NC, Bader AS, et al. Multisystem Imaging Manifestations of COVID-19, Part 1: Viral Pathogenesis and Pulmonary and Vascular System Complications. *Radiographics*. 2020;40(6):1574–1599. PMID: 33001783 https://doi.org/10.1148/rg.2020200149
53. Pershina ES, Cherniaev AL, Samsonova MV, Varyasin VV, Omarova ZR, Pereshivailov SO, et al. Comparison of the CT patterns and pulmonary histology in patients with COVID-19. *Medical Visualization*. 2020;24(3):37–53. (in Russ.) https://doi.org/10.24835/1607-0763-2020-3-37-53
54. Sulemane S, Baltabaeva A, Barron AJ, Chester R, Rahman-Haley S. Acute pulmonary embolism in conjunction with intramural right ventricular thrombus in a SARS-CoV-2-positive patient. *Eur Heart J Cardiovasc Imaging*. 2020;21(9):1054. PMID: 32338707 https://doi.org/10.1093/ehjci/jeaa115
55. Goswami U, Brenes JA, Punjabi GV, LeClaire MM, Williams DN. Associations and Outcomes of Septic Pulmonary Embolism. *Open Respir Med J*. 2014;8:28–33. PMID: 25184008 https://doi.org/10.2174/1874306401408010028 eCollection 2014.
56. Pelinovskaya LI. Features of the Modern Trend of Prosthetic and Electrode Endocarditis. *Siberian Medical Review*. 2015;(1):104–109. (in Russ.).

Received on 17.09.2021

Review completed on 25.11.2021

Accepted on 29.03.2022